Electronic Supplementary Material (ESI) for Physical Chemistry Chemical Physics.

Supporting Information for:

Dual mode quantitative imaging of microscopic viscosity using a conjugated porphyrin dimer

Aurimas Vyšniauskas,[a] Milan Balaz,[b]† Harry L. Anderson[b] and Marina K Kuimova[a*]

[a]Chemistry Department, Imperial College London, Exhibition Road, SW7 2AZ, UK
[b]Oxford University, Department of Chemistry, Chemistry Research Laboratory, Oxford, OX1 3TA, UK

Table of Contents

1. Derivation of lifetime-viscosity and ratio-viscosity relationship

The theoretical description of the viscosity-dependent photophysics was first suggested by Förster and Hoffmann.[5] The following dependency of quantum yield (φ_f) of molecular rotor on viscosity (η) of the solution was predicted:

$$\log \varphi_f = A + x \log \eta \quad (1)$$

φ_f is equal to:

$$\varphi_f = \frac{k_f}{k_f + k_{rot} + k_{nr}} \quad (2)$$

where k_f and k_{rot} are rate constants of fluorescence and non-radiative relaxation via rotation. k_{nr} is the sum of all other non-radiational decay constants. Fluorescence lifetime would be then equal to:

$$\tau = \frac{1}{k_f + k_{rot} + k_{nr}} \quad (3)$$

Combining equations 1 and 3 gives Förster-Hoffmann equation for fluorescence lifetime:

$\log \tau = x \log \eta + A - \log k_f$, or

$$\log \tau = x \log \eta + A' \quad (4)$$

where *A'* is a constant. According to Equation 4 a double logarithmic plot of lifetime versus viscosity should yield a straight line, which is not the case for **1** as seen in Figure 2c (main text). The fluorescence lifetime vs viscosity graph for **1** approaches an assymptotic value at high viscosities.

We hypothesise that this could be observed when the rate constant of rotational deactivation (i.e. 'molecular rotor' deactivation) becomes much smaller than the sum of all the other decay constants of deactivation. Such case cannot be described by Equation 4 because it implies that the fluorescence lifetime should always increase at increasing viscosity. Thus, the Förster-Hoffmann equation holds only when k_{rot} is the dominant or, at least, a significant decay constant and $k_{rot} > k_f + k_{nr}$.

In a case, where $k_{rot} >> k_f + k_{nr}$. fluorescence lifetime can be simplified to

$$\tau = \frac{1}{k_f + k_{rot} + k_{nr}} \approx \frac{1}{k_{rot}} \quad (5)$$

From Equations 4 and 5 k_{rot} is equal to

$$k_{rot} = \frac{\eta^{-x}}{A'} = A'' \eta^{-x} \quad (6)$$

In a case when k_{rot} is similar to k_f and k_{nr}, fluorescence lifetime is then equal to

$$\tau = \frac{1}{A"\eta^{-x} + k_{nr} + k_f} \tag{7}$$

At high viscosity A''η^{-x} term becomes negligible. Therefore, the highest achievable lifetime is

$$\tau_{\max} = \frac{1}{k_{nr} + k_f} \tag{8}$$

Since k_f and k_{nr} should be viscosity-independent constants, the following expression was used to fit lifetime calibration curve in Figure 2c:

$$\tau = \frac{1}{a_1 + a_2\eta^{a_3}} \tag{9}$$

where a_1, a_2 and a_3 are free fitting parameters.

The function (Eq 9) was also used for fitting the ratiometric calibration curve in Figure 2c.

2. Additional data

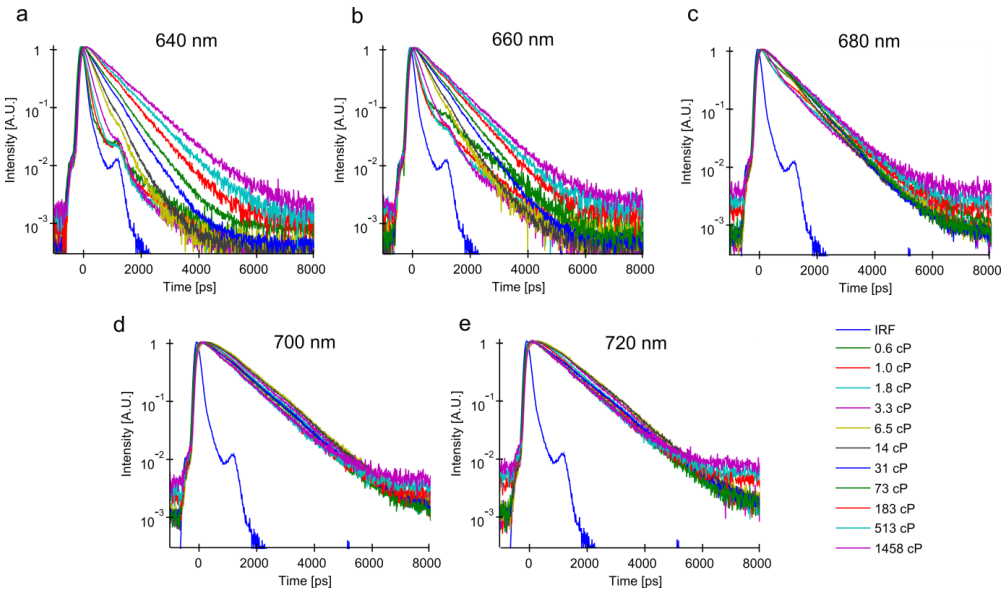

Figure S1. Normalized fluorescence decays of **1** in methanol glycerol mixtures of increasing viscosity. Emission wavelengths used for collecting decays are shown above the figure. It is clear to see that only the shorter wavelength decays show clear response to viscosity. These decays (640-660 nm) correspond to emission from the twisted conformer of **1**. The response to increasing viscosity of the 'planar' form of **1** is more subtle: increasing viscosity causes an increase in a risetime of these decay traces. Based on the data above we chose to use 635-650 nm window for the lifetime calibration of **1** against viscosity.

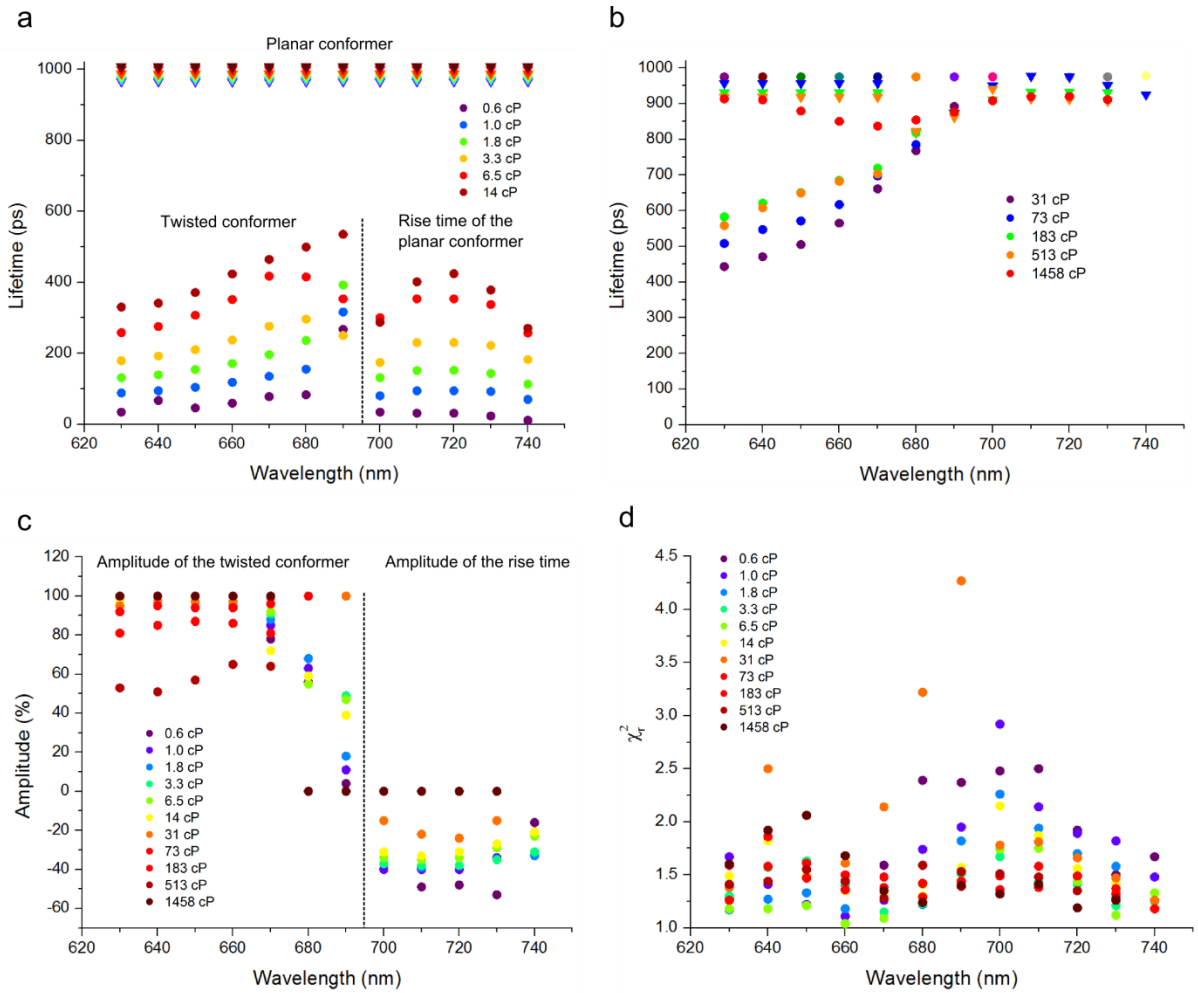

Figure S2. Biexponential fitting parameters of decay curves shown in Figure S1. (a) The fitted lifetimes obtained in 0.6 cP – 14 cP methanol/glycerol mixtures. The lifetimes were assigned to the twisted and planar conformers of **1** as shown in the Figure. The lifetime of the planar conformer was obtained by the fitting of the data at >700 nm where the planar decay is predominant and calculating the average lifetime. The planar lifetime was then fixed to a constant value for each dataset at a given viscosity. This allowed us to obtain a more reliable values for the second lifetime for decays below 700 nm. (b) The fitted lifetimes obtained in 31 cP – 1458 cP mixtures. Monoexponential fitting was done for 1458 cP data due to indistinguishable lifetime values of twisted and planar conformers. In these decays the rise time at >700 nm was not observed because of a low number of molecules converting from the originally excited twisted to the planar conformer at high viscosities. (c) Amplitudes corresponding to lifetimes of twisted conformer at <700 nm (positive values) and the rise time at >700 nm (negative values). Amplitudes of the twisted conformer were 95-100% below 670 nm in solutions with viscosity below 73 cP.

At higher viscosities similar lifetimes of both conformers are observed and this increases the error in fitting parameters. For viscosities above 73 cP, lifetime values for the calibration curve (Figure 2c, main text) were calculated using fixed amplitudes at 95% and 5%. (d) χ_r^2 parameters of all fits. High χ_r^2 at 670 – 700 nm was caused by significant overlaps between bands of planar and twisted conformers in which case triexponential model is required for obtaining a good fit. The data at these wavelengths was not used for calibration purposes.

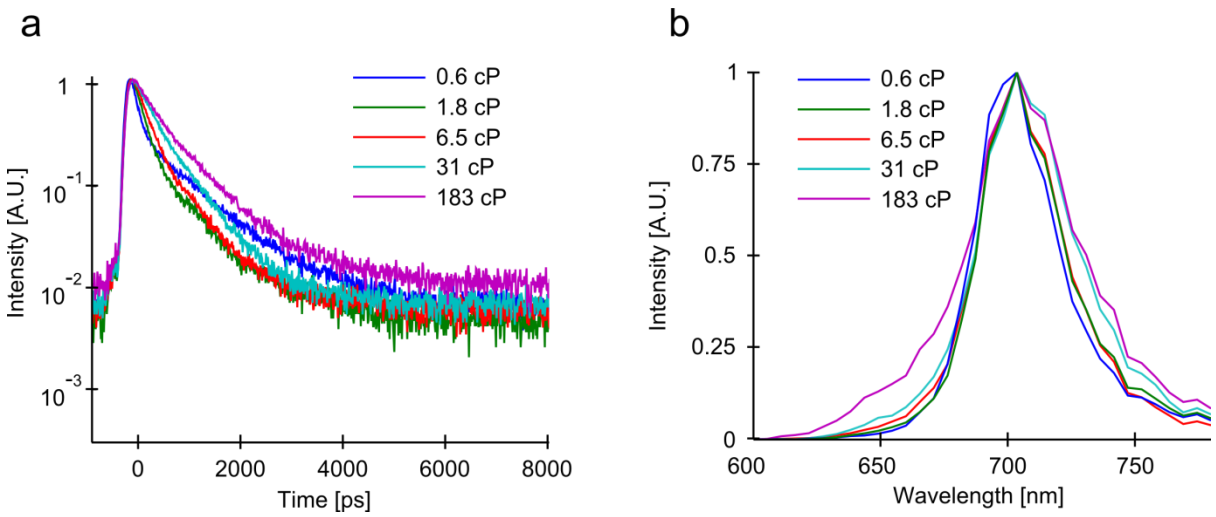

Figure S3. Two-photon excited (930 nm) fluorescence decays of **1** measured at 640 nm (a) and fluorescence spectra (b) obtained in methanol/ glycerol mixtures of varied viscosity. Both the decays and the spectra are dominated by the emission of the planar conformer of **1**, since much lower signal for the twisted conformer than in the case of the single photon excitation is observed. From this data we conclude that the molecular rotor **1** is not suitable for use with two photon excitation, possibly due to a preferential absorption of two-photon light by a more conjugated planar conformer.

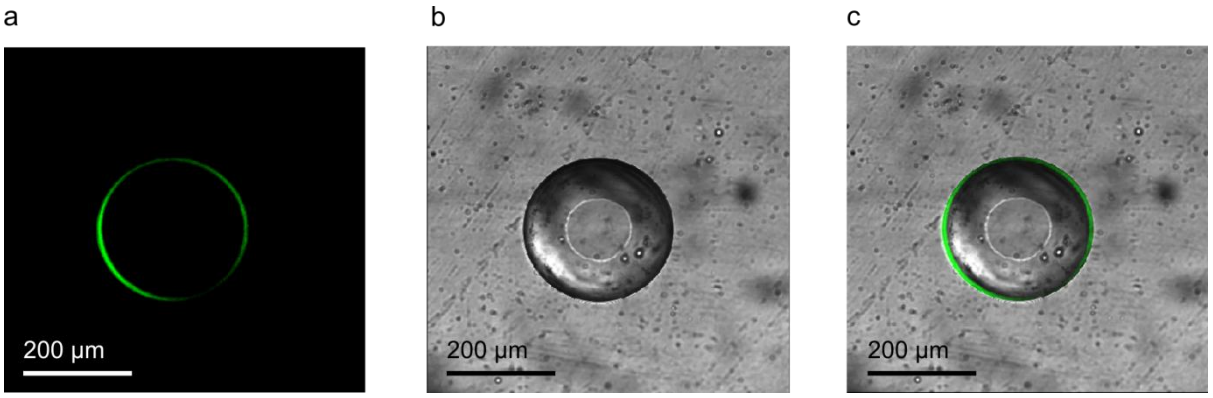

Figure S4. DPhPC monolayer created at a water/dodecane interface, incorporating **1;** λ_{exc} = 480 nm . (a) Fluorescence image. (b) Brightfield image. (c) Fluorescence and brightfield images merged. The clear polarisation-induced pattern is observed with top and bottom of the droplet appearing dark compared to the sides of the droplet.

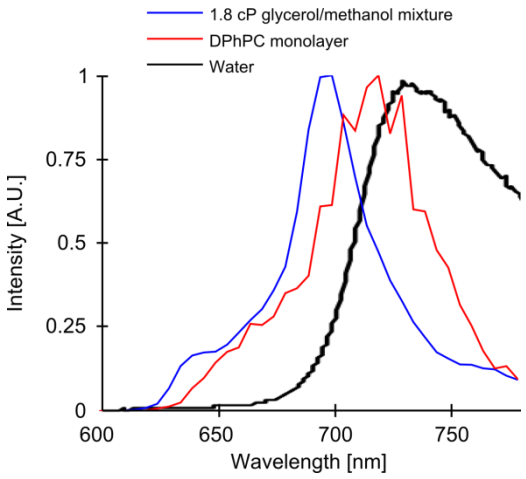

Figure S5. Fluorescence spectra of **1** recorded in environments of different polarity: 1.8 cP methanol /glycerol mixture (blue), DPhPC monolayer (red) and water (black). A clear red spectral shift is observed with increasing solvent polarity from methanol/glycerol (ε = ca 36) to water (ε = ca 81). The spectrum of **1** obtained in the monolayer displays an intermediate emission λ_{max} between the two solvents studied above.

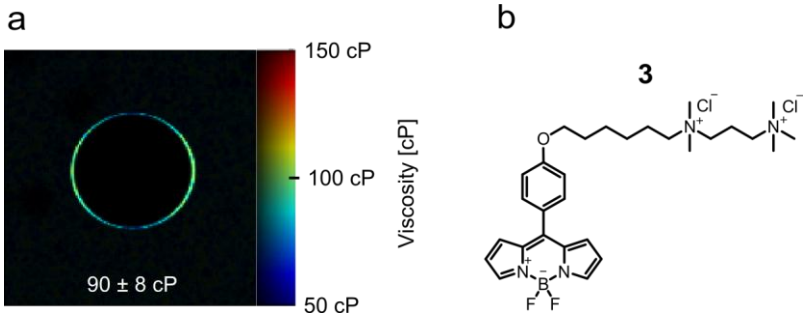

Figure S6. Viscosity map of DOPC monolayer (a) measured by Bodipy-class molecular rotor **3** (b).[6]

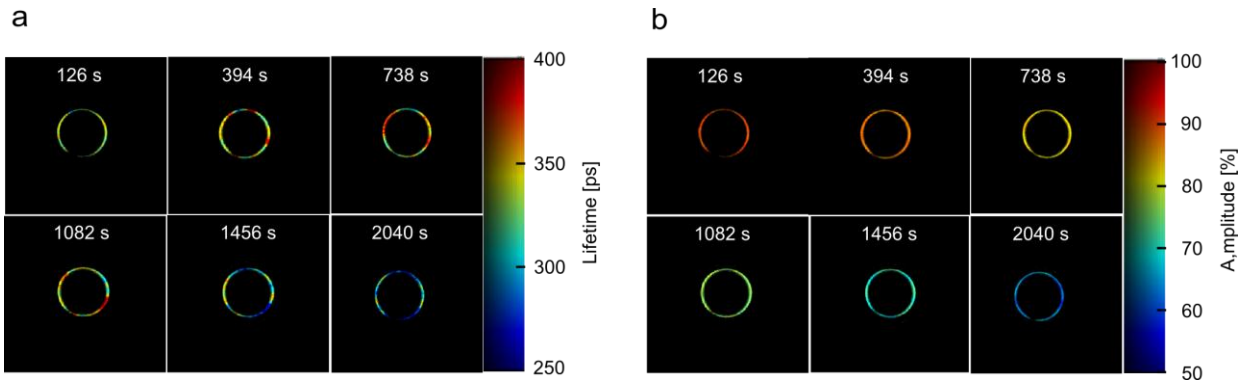

Figure S7. The lifetime (a) and the amplitude (b) maps of the twisted conformer of **1** in DOPC monolayer following irradiation at 453 nm. The duration of irradiation is shown in each image in white. The main change during irradiation is an increasing amplitude of the planar conformer, whereas the mean lifetime does not show significant changes. This data is further examined using the phasor approach, Figure S10.

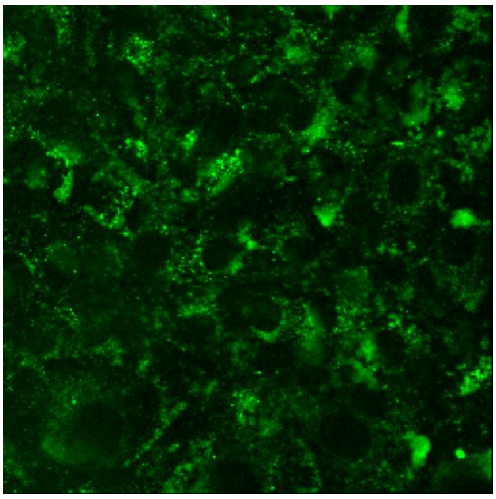

Figure S8. Confocal fluorescence image of SK-OV-3 cells stained with **1**; Excited at 453 nm, emission detected between 600 and 750 nm.

3. Phasor transforms of FLIM data in DPhPC monolayers and DOPC monolayers upon irradiation

Phasor analysis is a model-free analysis technique, which does not require any assumptions of a number of exponential components for the fitting.[7] The first step in the analysis is performing a Fourier transform of the fluorescence decay. The decay can be deconvoluted from the instrument response function (IRF) by dividing the Fourier transform of the decay by the Fourier transform of the IRF in the frequency domain.

The real and imaginary parts of the resulting value at a chosen frequency are plotted on the phasor plot. An example is shown in Figure S9, where three simulated decays are shown with their corresponding phasor transforms. A monoexponential decay gives a point on the semicircle, e.g. points shown in blue and green in Figure S9b. The position of points on the semicircle depends on the lifetime of the decay: a decay with longer lifetime will move counterclockwise on the semicircle compared to the shorter lifetime decay. E.g. the green point in Fig S9b has a longer lifetime than the blue point.

Any multiexponential decay will give a point somewhere within the semicircle. As a result, phasor transform allows distinguishing between monoexponential and multiexponential decays and gives an estimate of their lifetimes without any fitting required.

The phasor method can be extended to the analysis of FLIM images. As a result, every decay in the FLIM image will give a phasor point on the phasor diagram, e.g. Figure S9c. Phasor transform analysis does not require a prediction of the number of exponential components in mutiexponential decays before the analysis, which is a clear advantage in images with complex decays, such as collected in the case of **1** in lipid monolayers and bilayers.

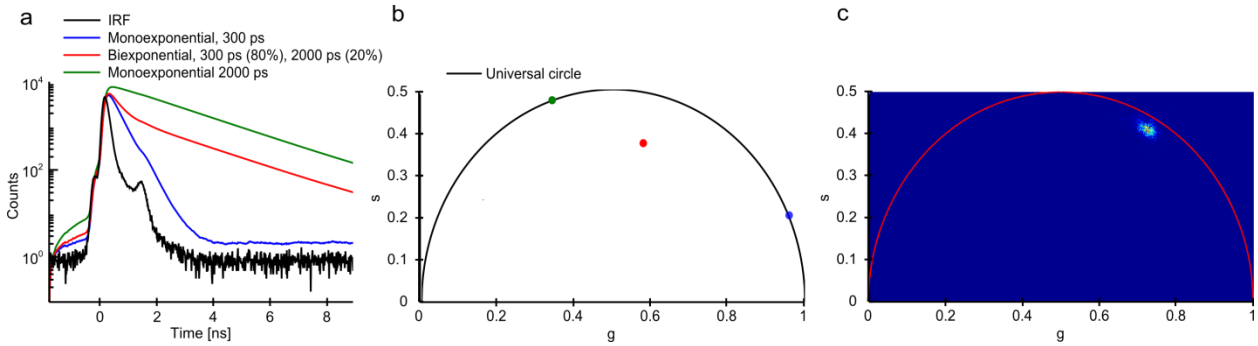

Figure S9. (a) Simulated decays, phasor transforms of which are shown in (b). Two monoexponential decays with 300 ps and 2000 ps lifetimes (blue and green, respectively) and biexponential decay with 50% amplitudes of 300 ps and 2000 ps lifetime (red) were simulated and convoluted with experimental IRF (black). (c) An example of phasor transform of a FLIM image.

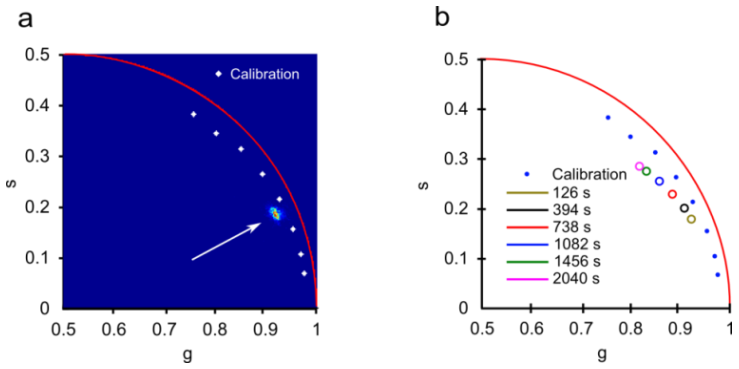

Figure S10. (a) Phasor transforms of the calibration data of **1** in methanol/glycerol mixtures, which were reported in the main text Figure 2b (white dots). Phasor transform of FLIM image reported in Figure 3a (main text) is indicated by a white arrow. It could be seen that the phasor cloud of a monolayer image lies significantly further away from the semicircle than the phasor points of individual calibration decays, which is consistent with a stronger biexponential character of the decays recorded in a monolayer. (b) Phasor transform of FLIM images of **1** in DOPC monolayers at different irradiation times. Centres of the clouds are shown as circles for clarity. Blue dots are calibration data. A trajectory upwards and to the left with irradiation time is seen, indicating increasing viscosity.

4. References

1. Balaz, M., Collins, H. A., Dahlstedt, E. & Anderson, H. L. Synthesis of hydrophilic conjugated porphyrin dimers for one-photon and two-photon photodynamic therapy at NIR wavelengths. *Org. Biomol. Chem.* **7,** 874–888 (2009).

2. Holden, M. a, Needham, D. & Bayley, H. Functional bionetworks from nanoliter water droplets. *J. Am. Chem. Soc.* **129,** 8650–5 (2007).

3. Angelova, M. I. & Dimitrov, D. S. Liposome Electro formation. 303–311 (1986).

4. Warren, S. C. *et al.* Rapid global fitting of large fluorescence lifetime imaging microscopy datasets. *PLoS One* **8,** e70687 (2013).

5. Forster, T. & Hoffmann, G. Viscosity Dependence of Fluorescent Quantum Yields of Some Dye Systems. *Zeitschrift Fur Phys. Chemie-Frankfurt* **75,** 63–& (1971).

6. López-Duarte, I., Vu, T. T., Izquierdo, M. A., Bull, J. a & Kuimova, M. K. A molecular rotor for measuring viscosity in plasma membranes of live cells. *Chem. Commun. (Camb).* **50,** 5282–4 (2014).

7. Digman, M. a, Caiolfa, V. R., Zamai, M. & Gratton, E. The phasor approach to fluorescence lifetime imaging analysis. *Biophys. J.* **94,** L14–6 (2008).